For Supporting Information:

# Synthesis, Structure and Molecular Modelling of Anionic Carbosilane Dendrimers

**Beatriz Rasines,[a] Javier Sánchez-Nieves,[a] Massimo Maiolo,[b] Marek Maly,[b,c] Louis Chonco,[d] José Luis Jiménez,[e] M. Ángeles Muñoz-Fernández,[d] F. Javier de la Mata[a,*] and Rafael Gómez[a,*]**

rafael.gomez@uah.es

**RECEIVED DATE (to be automatically inserted after your manuscript is accepted if required according to the journal that you are submitting your paper to)**

[a] Dpto. de Química Inorgánica, Universidad de Alcalá, Campus Universitario, E-28871 Alcalá de Henares (Madrid) Spain. FAX: 00 34 91 885 4683; Phone: 00 34 91 885 4685. Networking Research Center on Bioengineering, Biomaterials and Nanomedicine (CIBER-BBN).

[b] University of Applied Science of Southern Switzerland, Department of Innovative Technologies. SUPSI-DTI Galleria 2, CH-6928 Manno, Switzerland.

[c] Faculty of Science, J. E. Purkinje University, Ceske mladeze 8, 400 96 Usti n. L., Czech Republic.

[d] Laboratorio de Inmunología Molecular, Hospital General Universitario Gregorio Marañón, Madrid (Spain). Networking Research Center on Bioengineering, Biomaterials and Nanomedicine (CIBER-BBN).

[e] Plataforma de Laboratorio, Hospital General Universitario Gregorio Marañón, Madrid (Spain). Networking Research Center on Bioengineering, Biomaterials and Nanomedicine (CIBER-BBN), Spain.

-BBN), Spain.

## Interaction of anionic dendrimers with $Na^+$ cations

As we can see on Figure 5E (from main text), one narrow peak is observed whose center is located at 2.35 Å and dominates to all six profiles. This fact means that the most frequently occupied distance of $Na^+$ ions respect to terminal oxygens is in both cases ($CO_2^-$, $SO_3^-$) 2.35 Å. However, the peaks belonging to sulfonate-terminated dendrimers are almost identical (not influenced by dendrimer core) and significantly smaller than that obtained for the non-protonated carboxylate structures. Density maxima obtained from carboxylate dendrimers (non-protonated) differ and the height of phenoxo cored dendrimer peak is 1.57 times bigger than in case of the Si cored one. The above observations indicate stronger interaction of $Na^+$ ions with carboxylate surface where stronger one-to-one interaction of $Na^+$ ions with individual $CO_2$ groups is combined with better ability of cooperative stabilization of $Na^+$ ions with these terminal groups (see Figure S6 in Supporting Information). Moreover, this cooperative stabilization is better in case of polyphenoxo cored Dendrimer with $CO_2$ units than in case of Si cored ones, partially explaining the difference between profiles of dendrimers **8** and **11**. In addition, as it was proved by our short additional simulations with rigid (constrained) structures the flexibility of $CO_2$ groups is not as important here as their previously established distribution and mutual orientation on dendrimer surface which was anyway achieved with partial contribution of strong $Na^+ \ldots CO_2^-$ one-to-one interaction. This active role of $Na^+$ ions in the surface could be also seen from the existence of the mutual oxygen radial density maxima located *ca.* at 4 Å, which is evident especially in case of non-protonized dendrimer **8** while in case of protonated version **8p** this maximum disappeared as there are no close $Na^+$ ions which could be able to induce relevant $CO_2$-$CO_2$ configurations (see Figures 5F and S6 in Supplementary Information). The stronger interaction of $Na^+$ ions with non-protonated $CO_2$ terminated dendrimers may also partially explain their slightly smaller size and surface comparing to the sulfonate or protonated carboxylate ones (see Table 1). The presence of more and/or more stable $Na^+$ ions in close proximity of dendrimer surface might more effectively contributes to the screening of the dendrimer surface charge ($Na^+$ ions may even act here as some effective internal glue). This feature may induce a little more compact and therefore also slightly smaller stucture. Another partial contributions regarding the measured differences in size may come also from differences in N-$CO_2$, N-$SO_3$ ( *ca.* 1.5 Å, 1.8 Å) and C-O, S-O (*ca.* 1.1 Å, 1.4 Å) bond lengths.

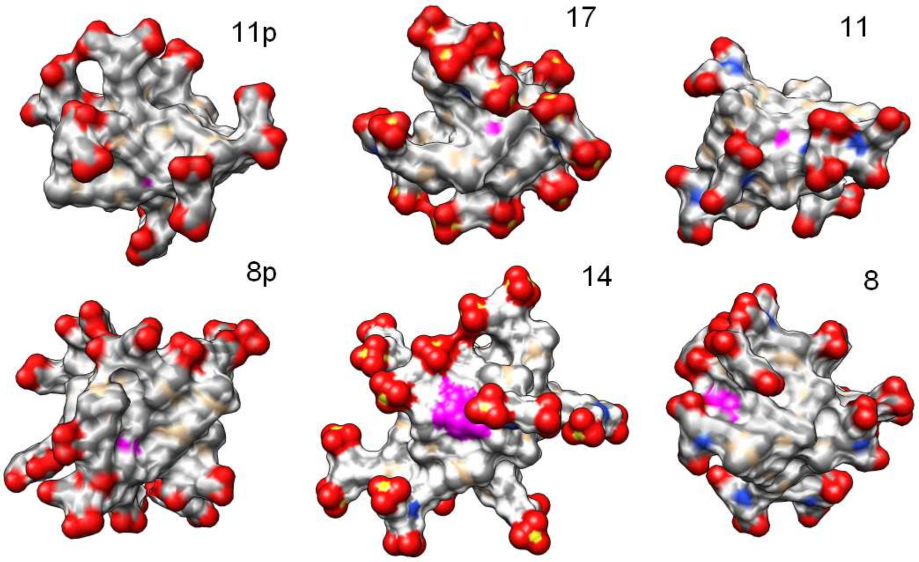

**Figure S1.** Computer models of dendrimers **8**, **11**, **14** and **17** simulated in salt water with visualized molecular surfaces. Dendrimers labeled as **8p**, **11p** are dendrimers **8** and **11** with protonated nitrogens but deprotonated peripheral anionic groups. The dendrimer core is colored in magenta.

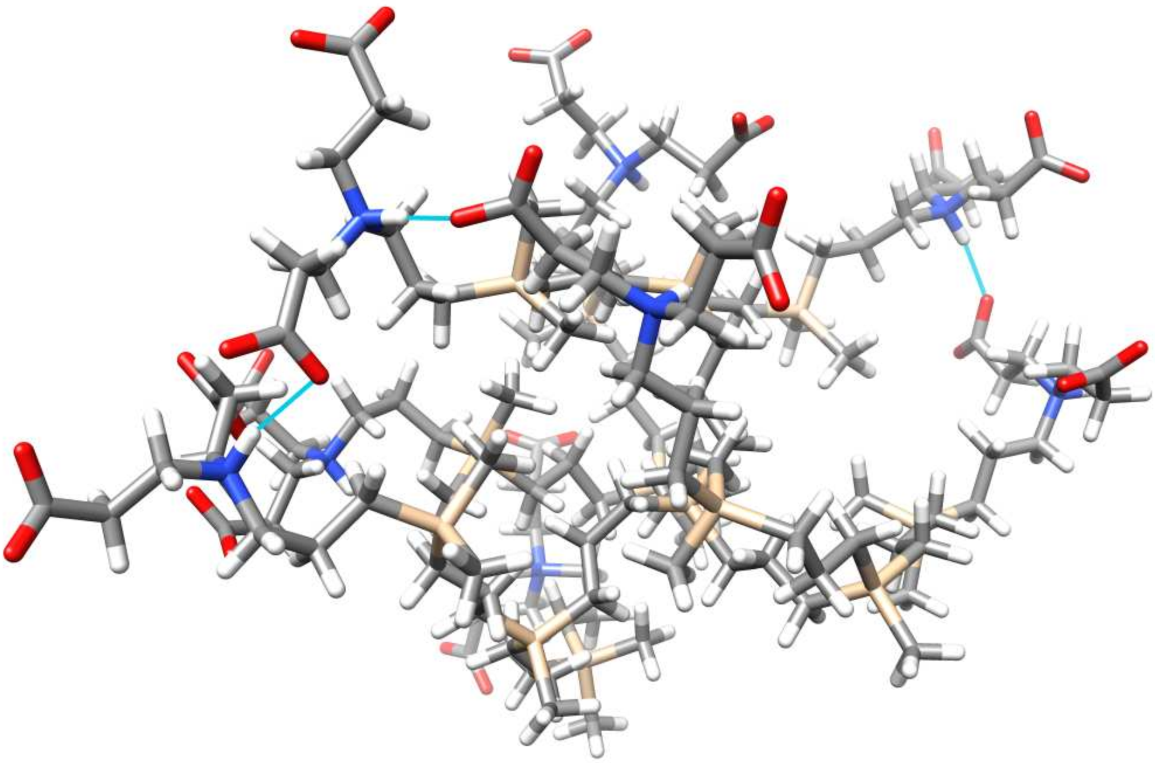

**Figure S2**. Visualization of dendrimer **11p** including 3 intra-molecular hydrogen bonds (or more precisely salt bridges) which are coloured in cyan.

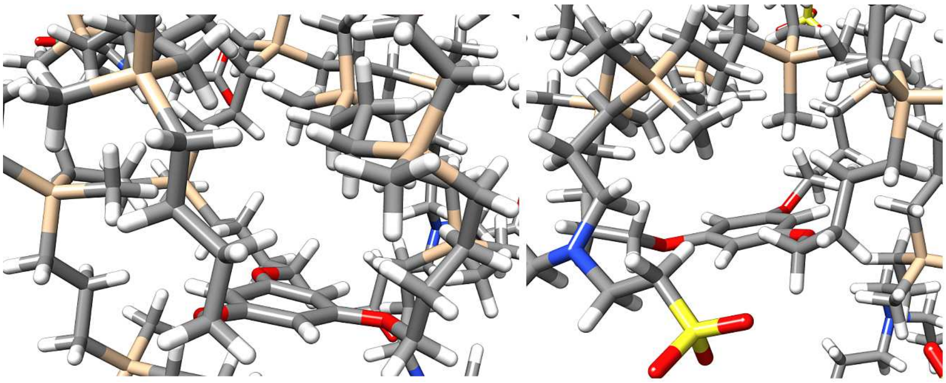

**Figure S3.** View of the small internal cavities within the carboxylate-terminated (left) and sulfonate-terminated (right) polyphenoxo cored dendrimers.

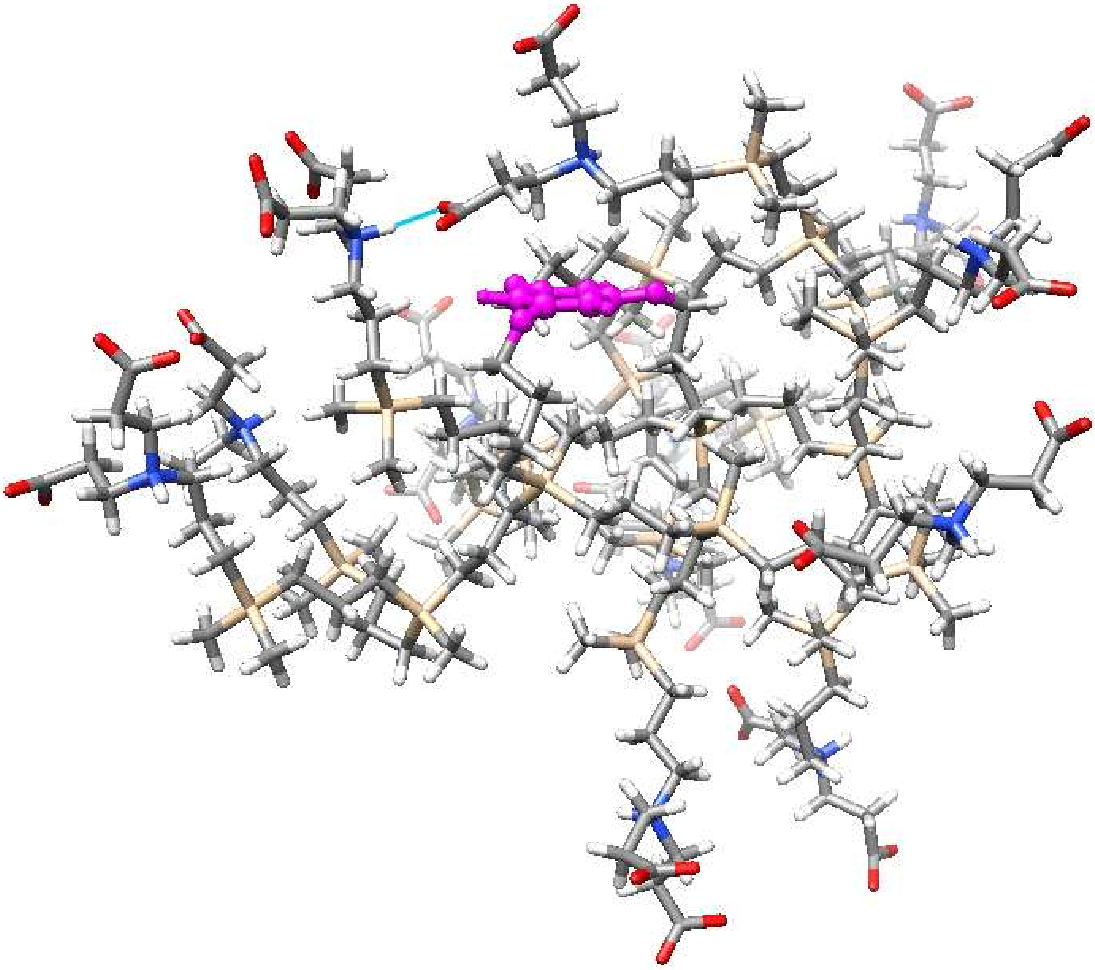

**Figure. S4**. Backfolding in case of dendrimer **8p** supported with NH…O hydrogen bond (in cyan). Dendrimer core is highlighted with magenta color.

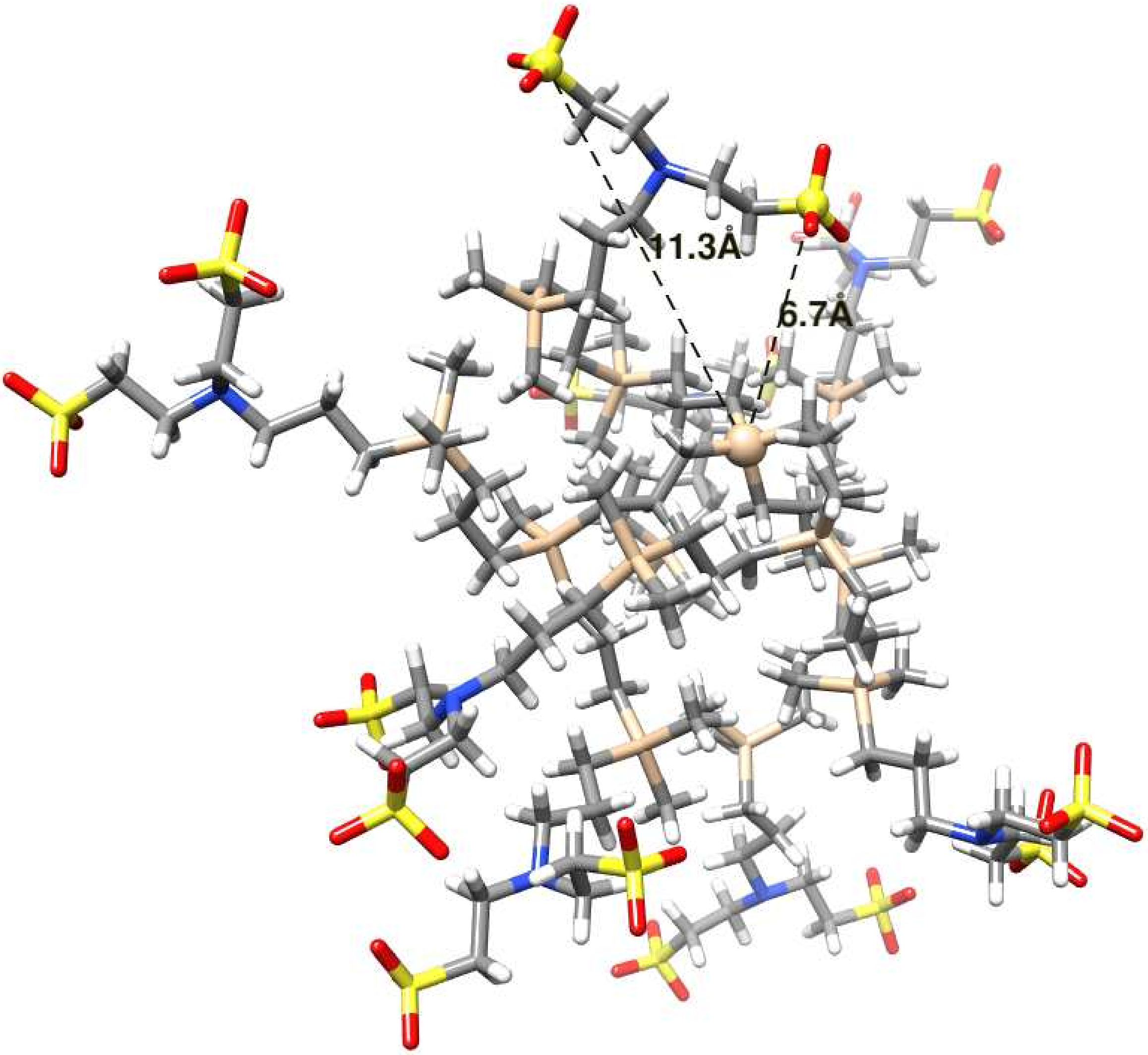

**Figure S5**. Illustration of back-folding in case of dendrimer **17**. Si core atom is in “sphere” representation.

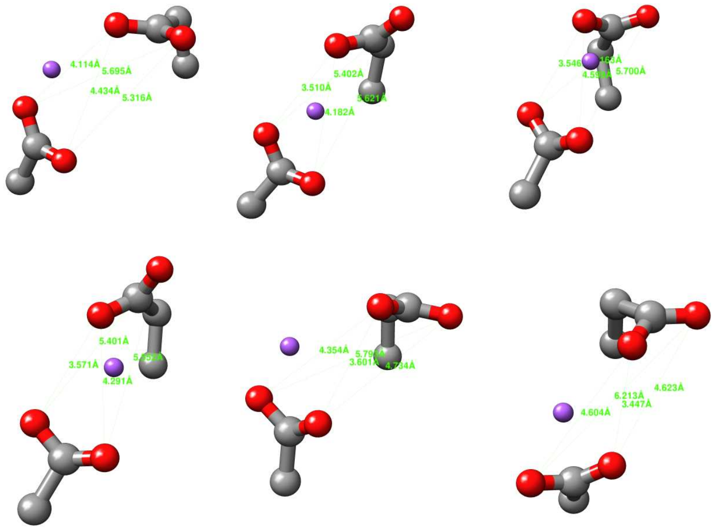

**Figure S6**. Six configurations of the same $CO_2$ pair from the dendrimer **8** surface coordinating $Na^+$ ion. The configurations were obtained at the end of the simulation in order: top-left -> top-right -> bottom-left -> bottom-right. Each two neighbouring snapshots (with respect to the order) are separated with 25000 of 2 fs steps (50 ps) so the time interval between the first and the last frame is 0.3 ns.The small numbers denotes the mutual distances of oxygen atoms which span distances from *ca* 3.5 Å to 6 Å.

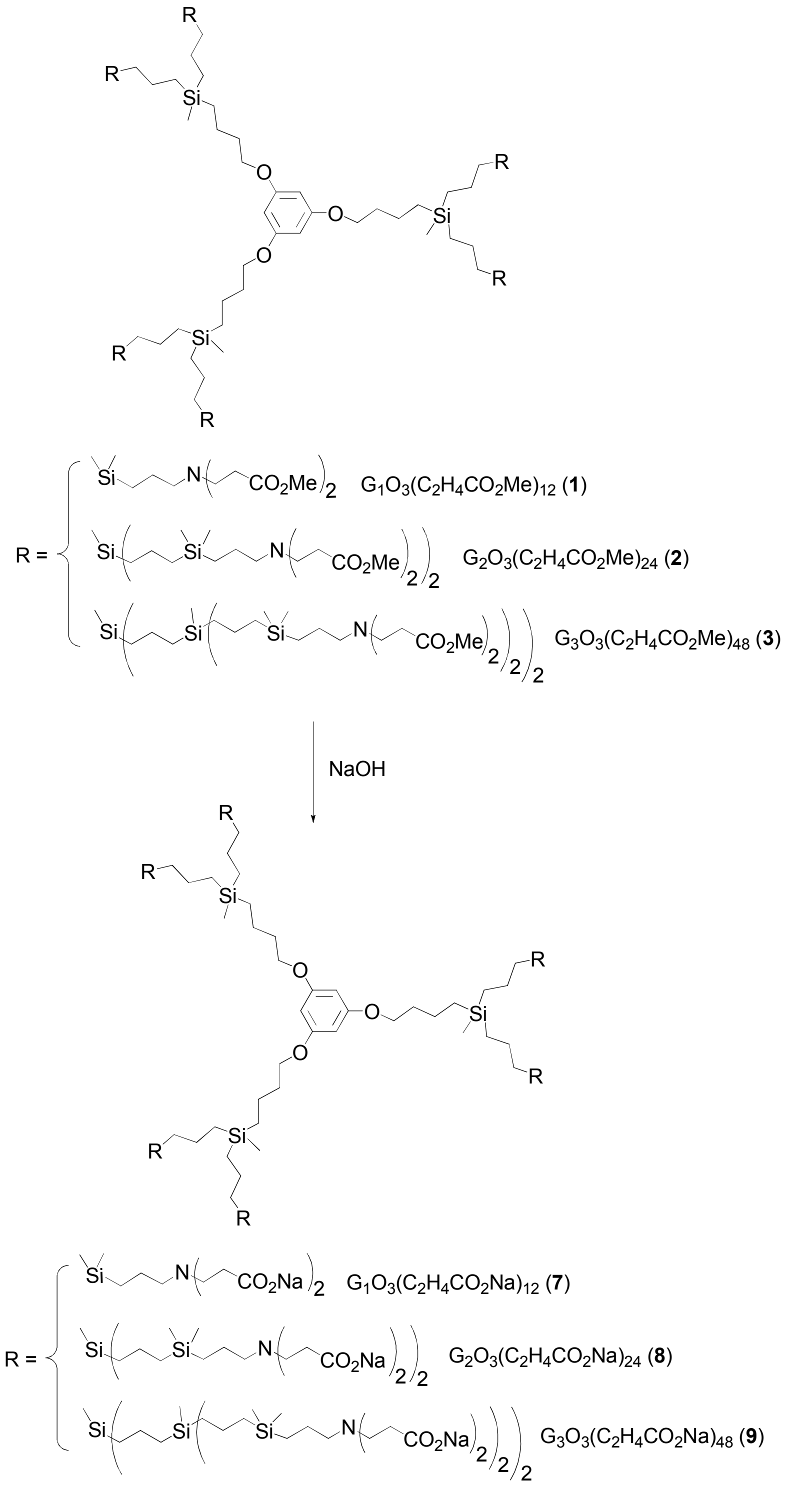

$G_1O_3(C_2H_4CO_2Me)_{12}$ (**1**)

$G_2O_3(C_2H_4CO_2Me)_{24}$ (**2**)

$G_3O_3(C_2H_4CO_2Me)_{48}$ (**3**)

$G_1O_3(C_2H_4CO_2Na)_{12}$ (**7**)

$G_2O_3(C_2H_4CO_2Na)_{24}$ (**8**)

$G_3O_3(C_2H_4CO_2Na)_{48}$ (**9**)

**Scheme S7**. Synthesis of anionic dendrimers **7-9**.

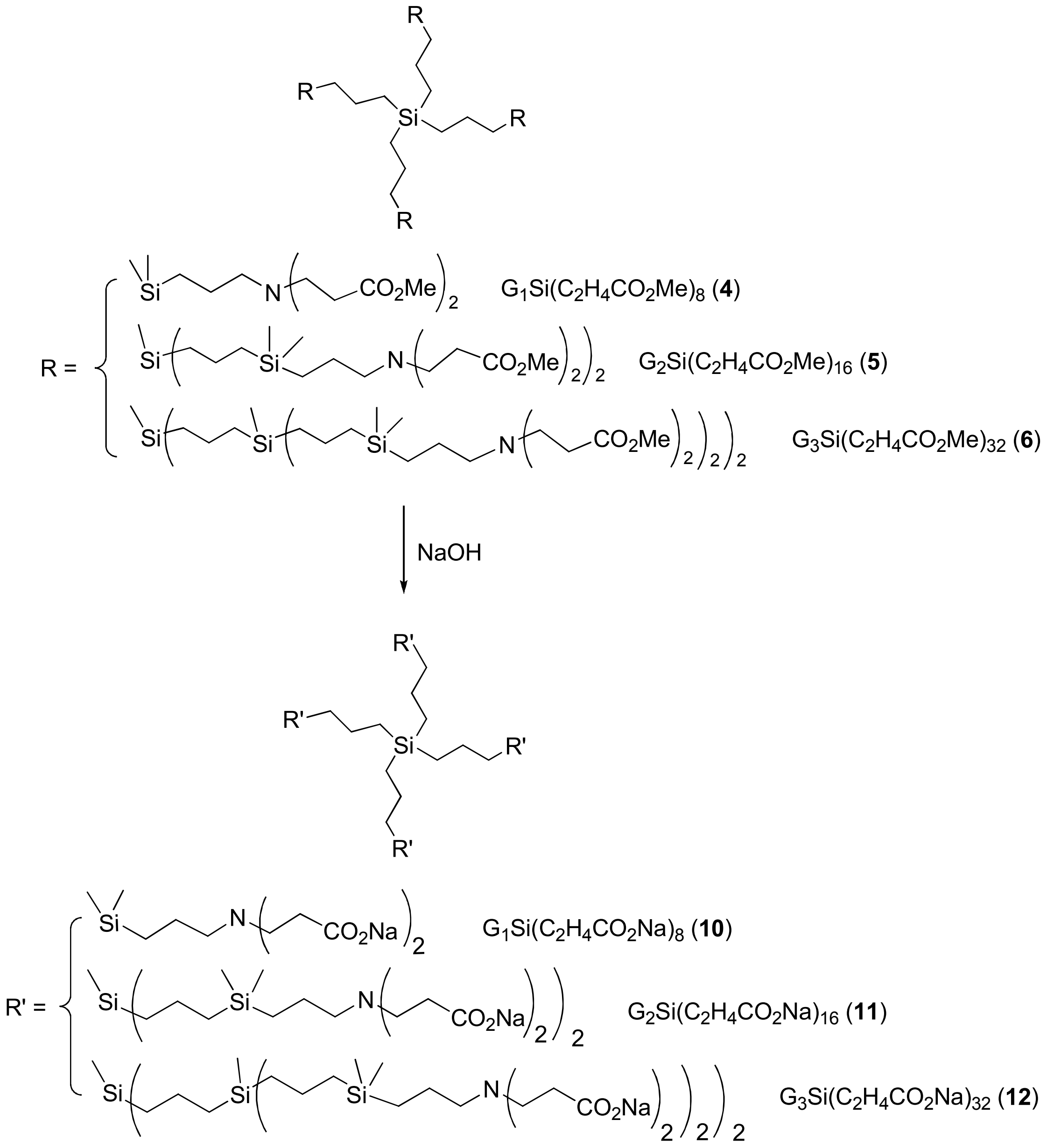

**Scheme S8**. Synthesis of anionic dendrimers **10-12**.

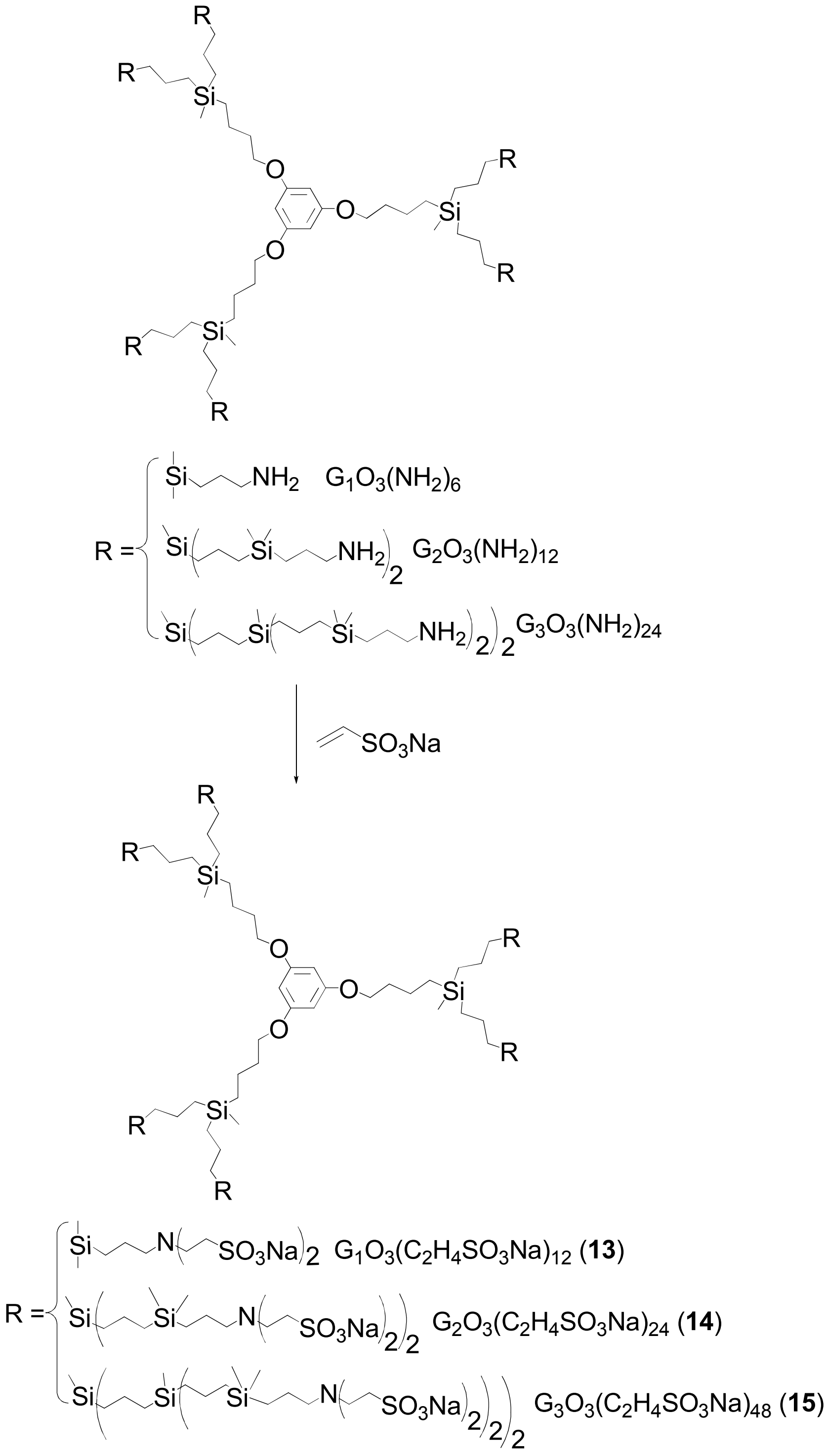

**Scheme S9**. Synthesis of anionic dendrimers **13-15**.

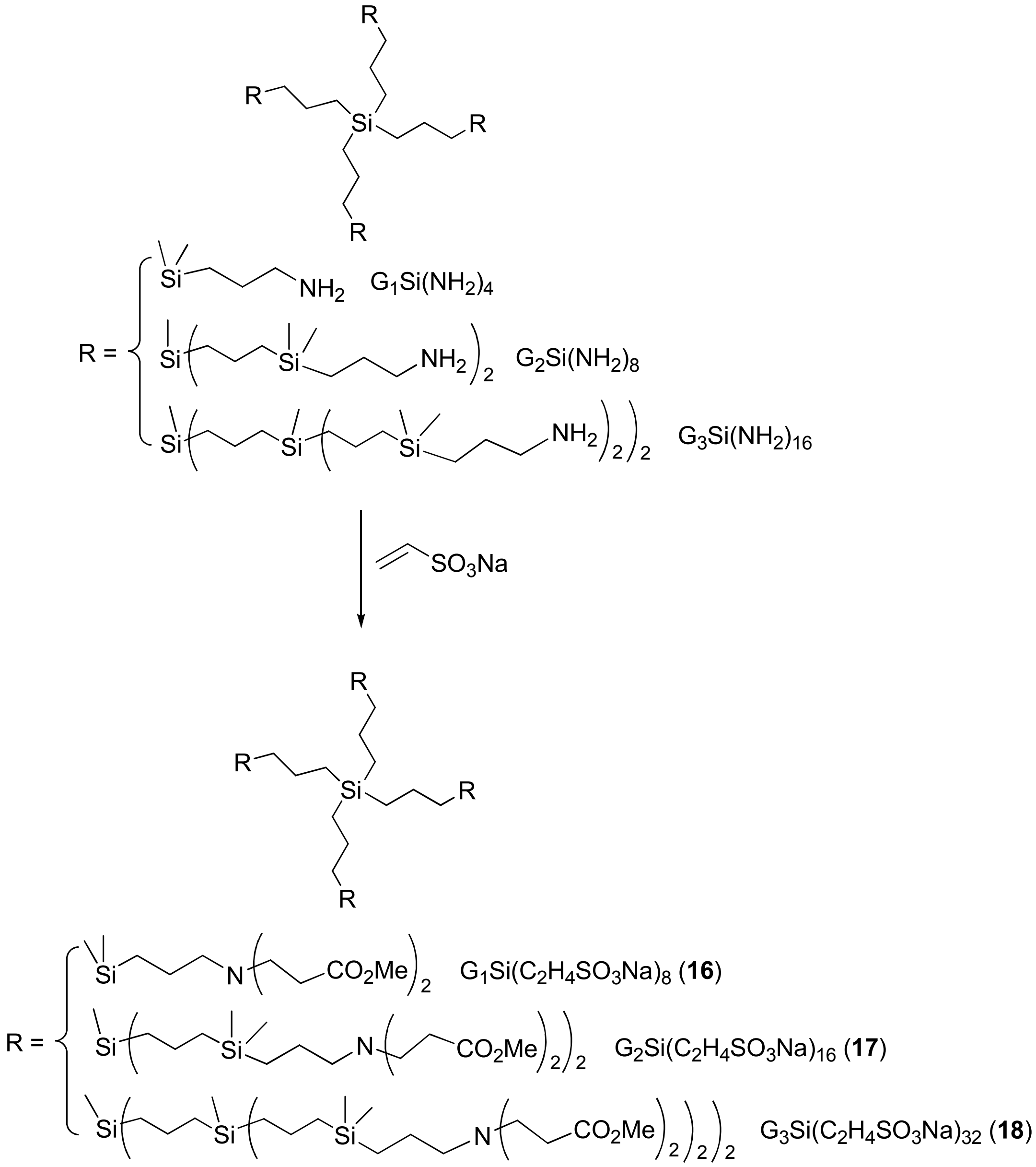

**Scheme S10**. Synthesis of anionic dendrimers **16-18**.

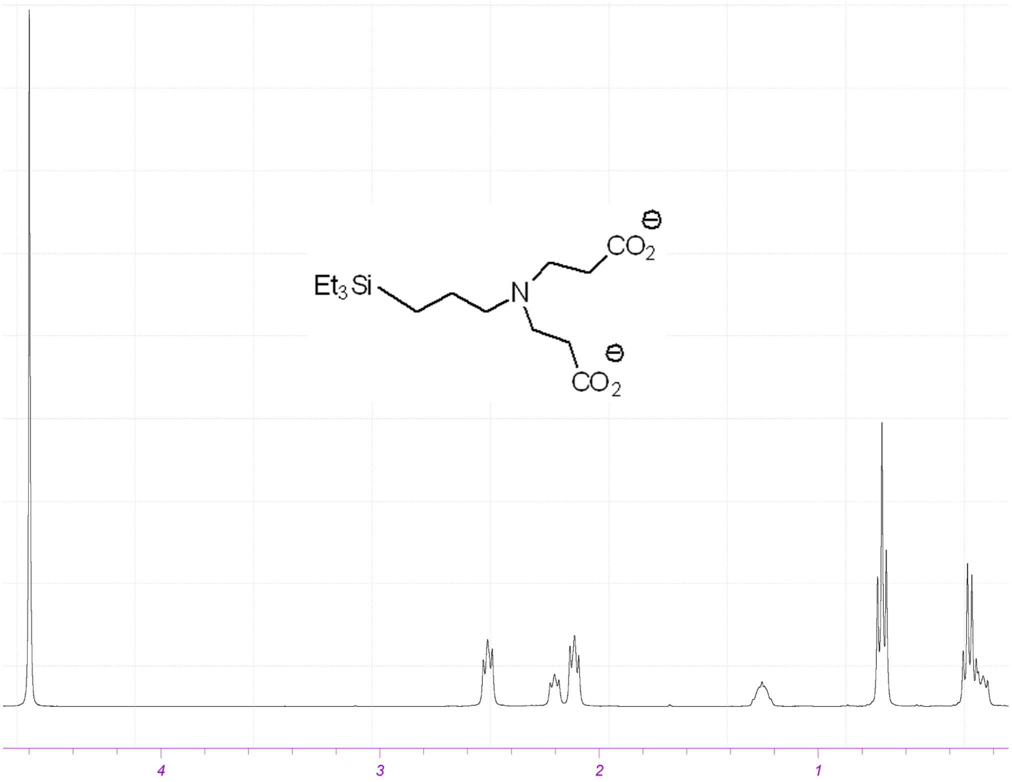

**Figure S11**. $^1$H NMR spectrum of $G_0N(CO_2Na)_2$ (**B**).

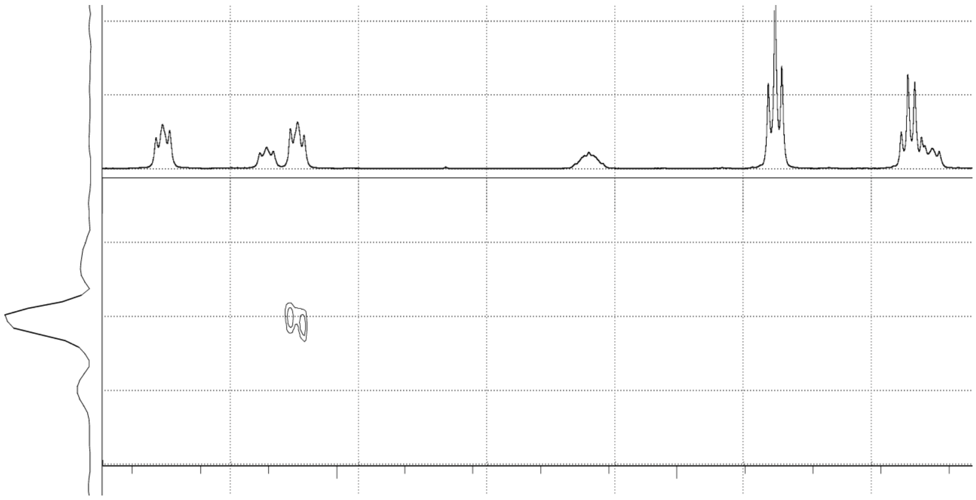

**Figure S12**. $^{15}$N NMR spectrum of $G_0N(CO_2Na)_2$ (**B**).

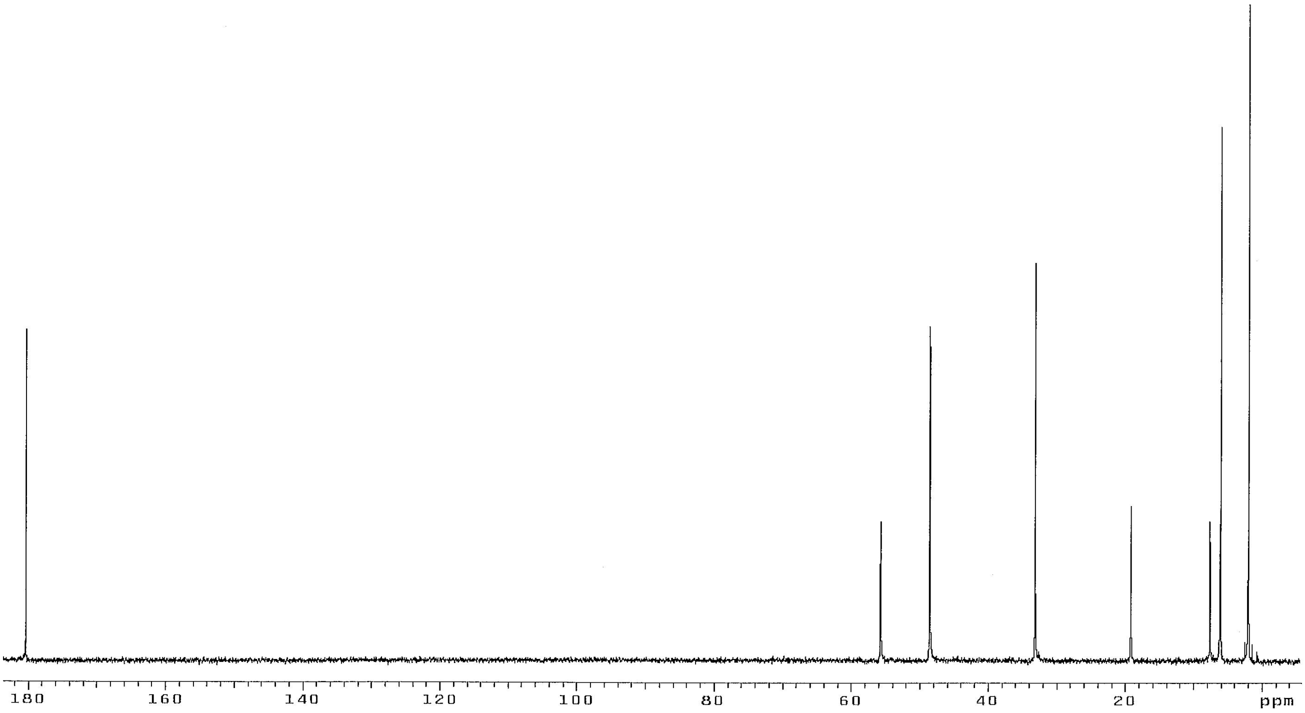

**Figure S13**. $^{13}$C NMR spectrum of $G_0N(CO_2Na)_2$ (**B**).

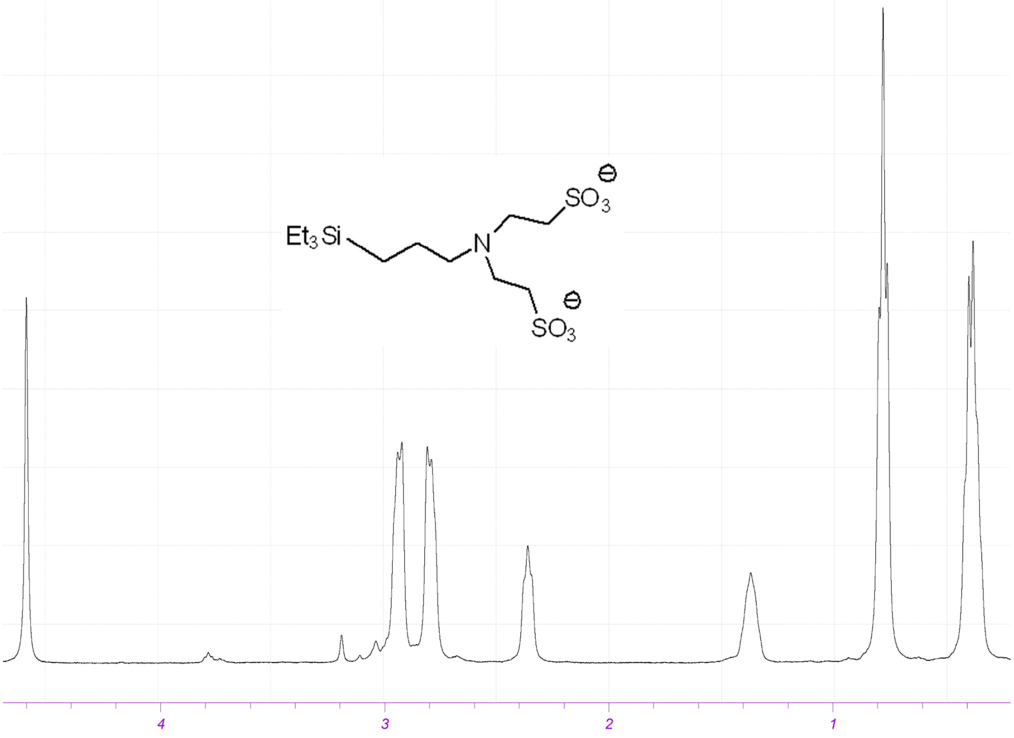

**Figure S14**. $^{1}$H NMR spectrum of $G_0N(SO_3Na)_2$ (**D**).

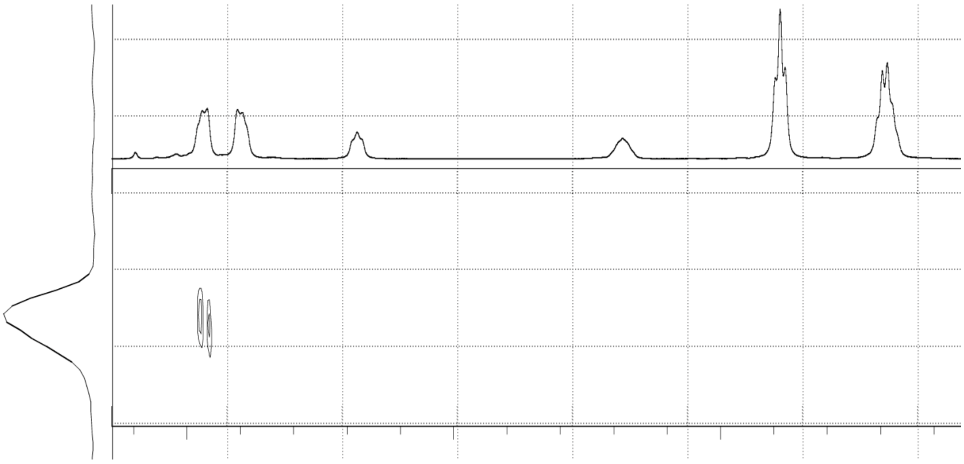

**Figure S15**. $^{15}N$ NMR spectrum of $G_0N(SO_3Na)_2$ (**D**).

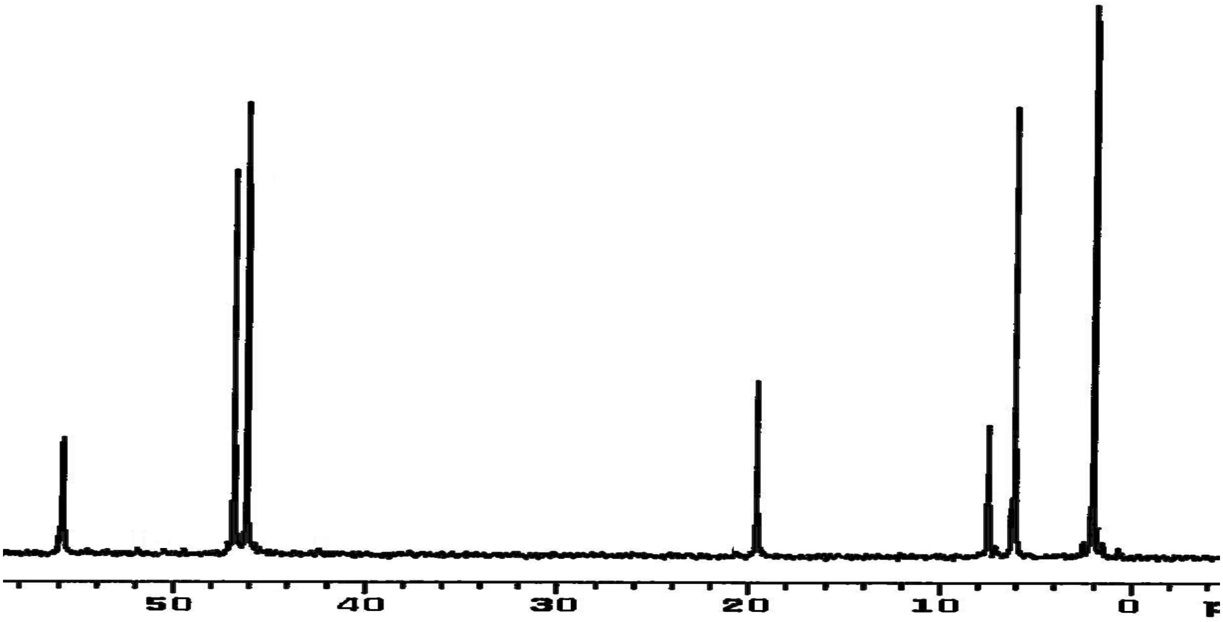

**Figure S16**. $^{13}C$ NMR spectrum of $G_0N(SO_3Na)_2$ (**D**).

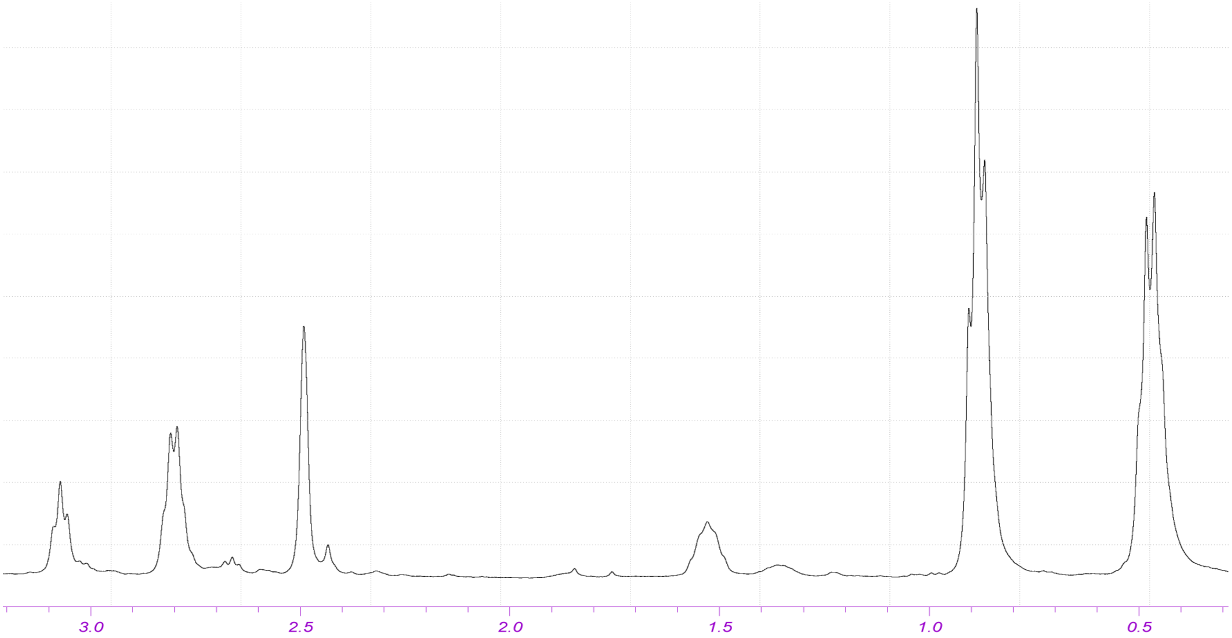

**Figure S17**. $^{1}$H NMR spectrum of $G_0NH(SO_3Na)$ (**E**).

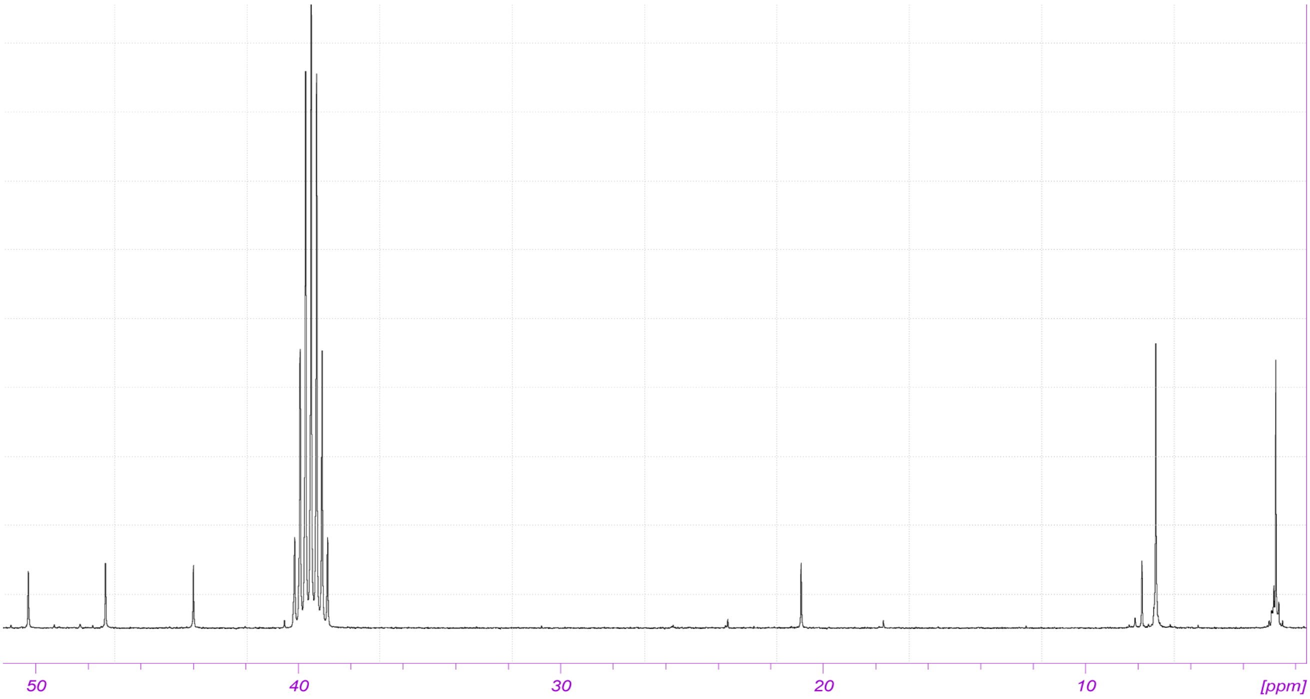

**Figure S18**. $^{13}$C NMR spectrum of $G_0NH(SO_3Na)$ (**E**).

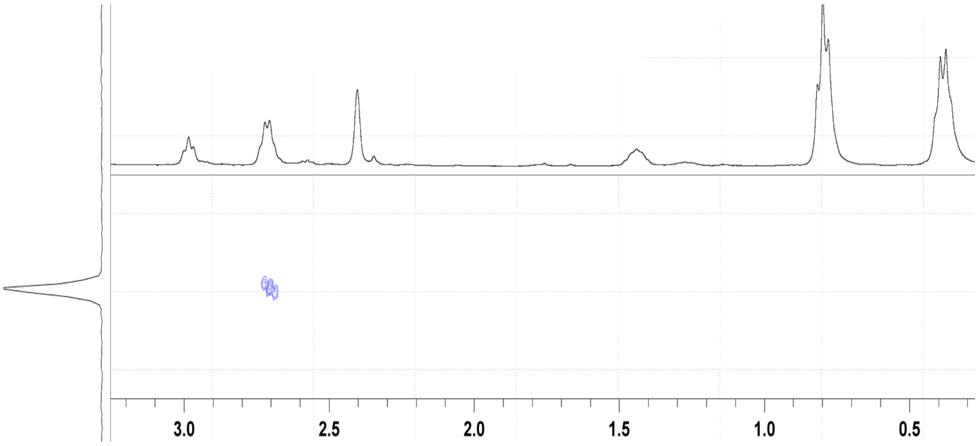

**Figure S19**. $^{15}N$ NMR spectrum of $G_0NH(SO_3Na)$ (**E**).

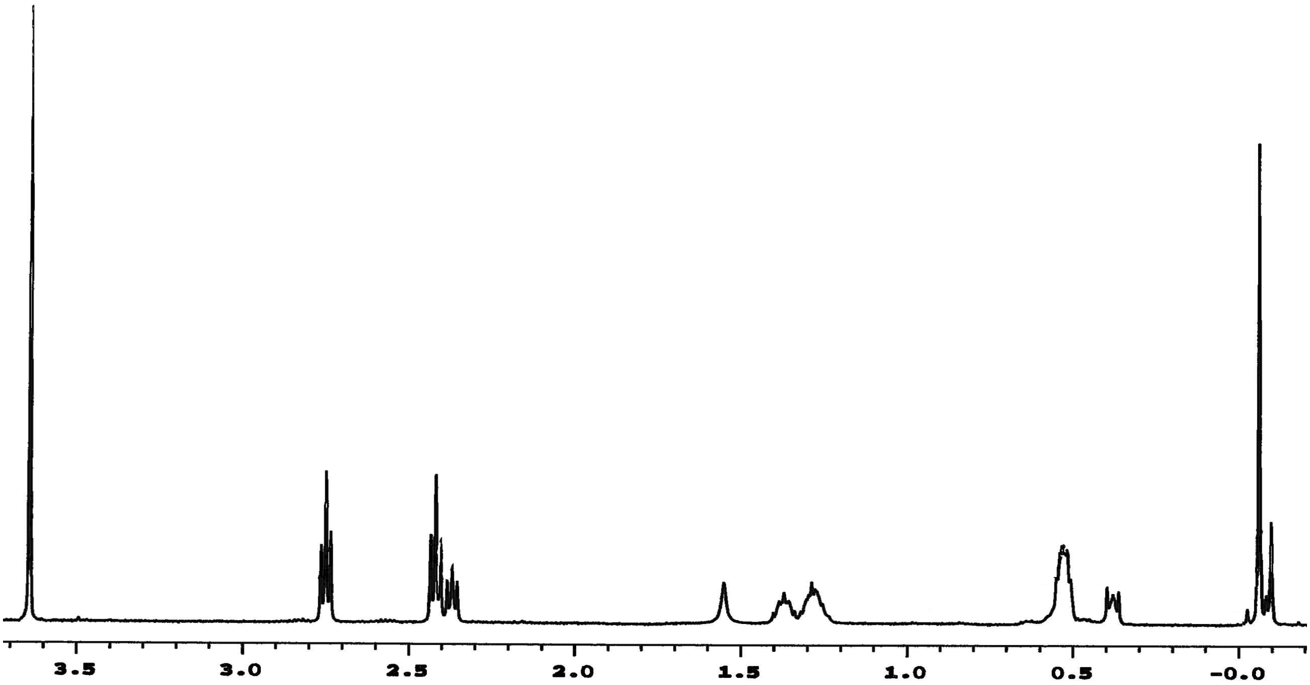

**Figure S20**. $^1H$ NMR spectrum of $G_2Si(C_2H_4CO_2Me)_{16}$ (**5**).

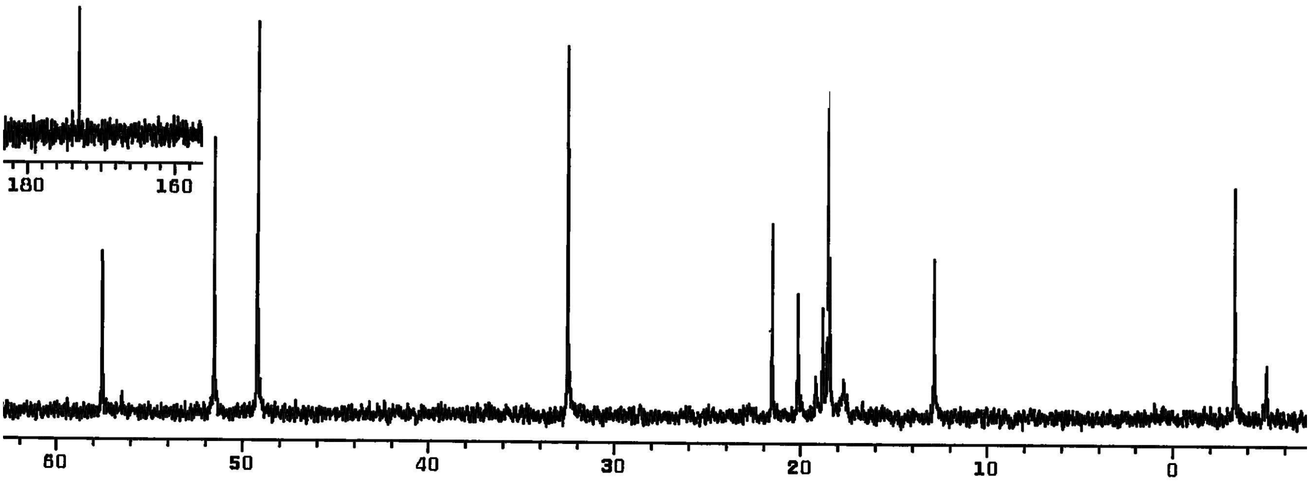

**Figure S21**. $^{13}$C NMR spectrum of $G_2Si(C_2H_4CO_2Me)_{16}$ (**5**).

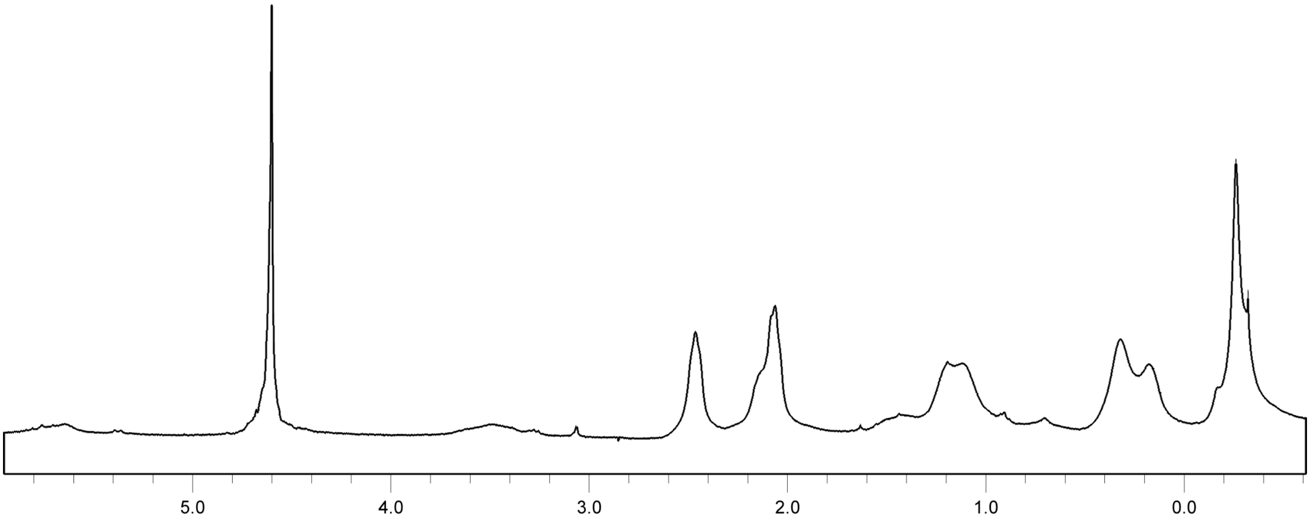

**Figure S22**. $^{1}$H NMR spectrum of $G_1O_3(C_2H_4CO_2Na)_{12}$ (**7**).

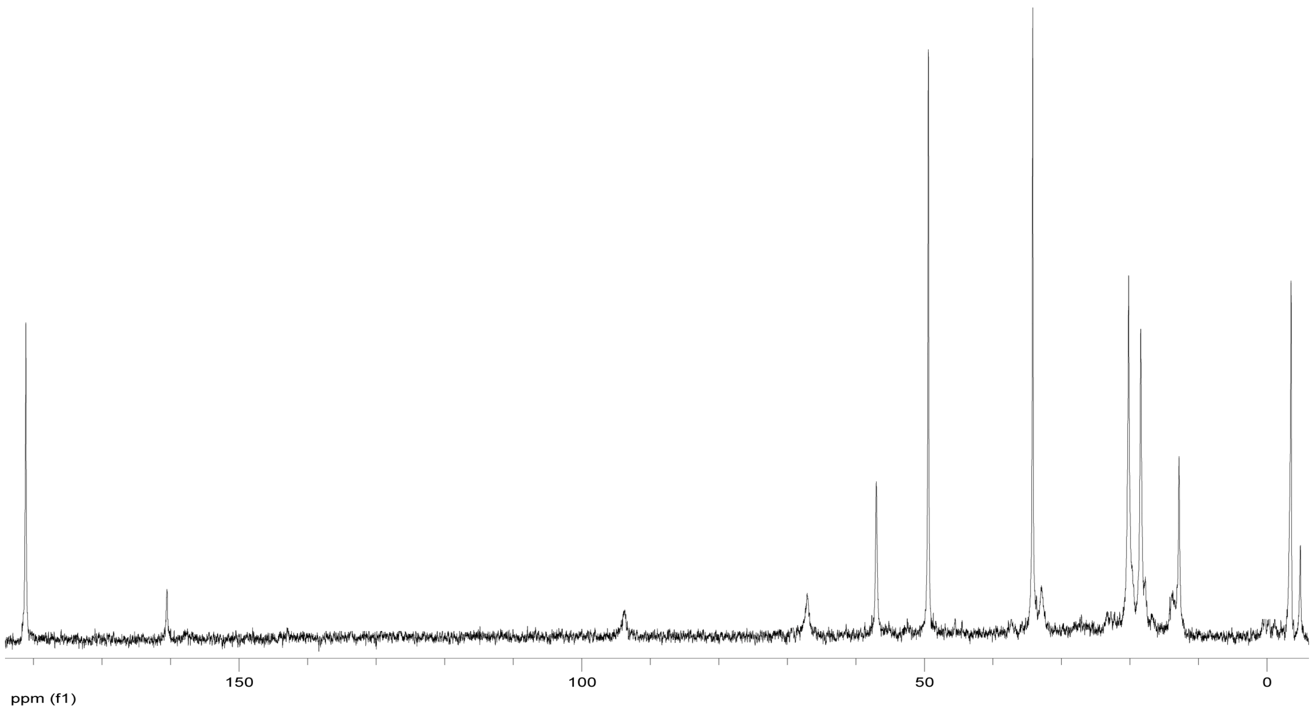

**Figure S23**. $^{13}C$ NMR spectrum of $G_1O_3(C_2H_4CO_2Na)_{12}$ (**7**).

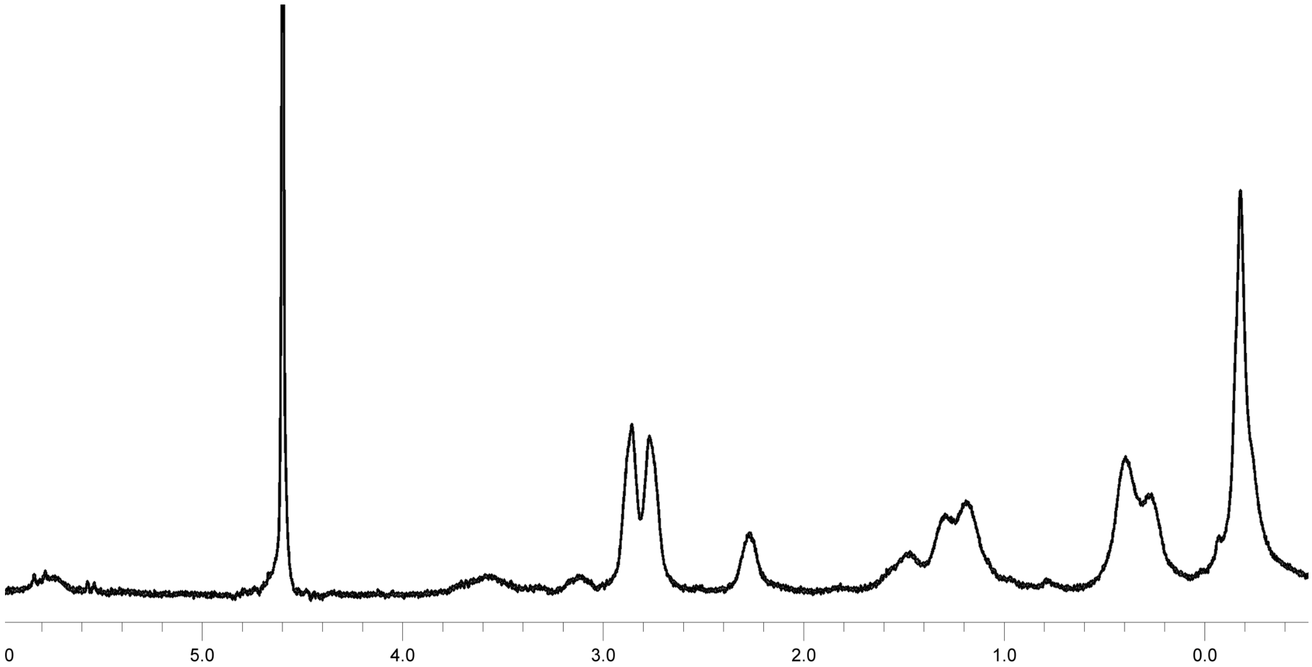

**Figure S24**. $^{1}H$ NMR spectrum of $G_1O_3(C_2H_4SO_3Na)_{12}$ (**13**).

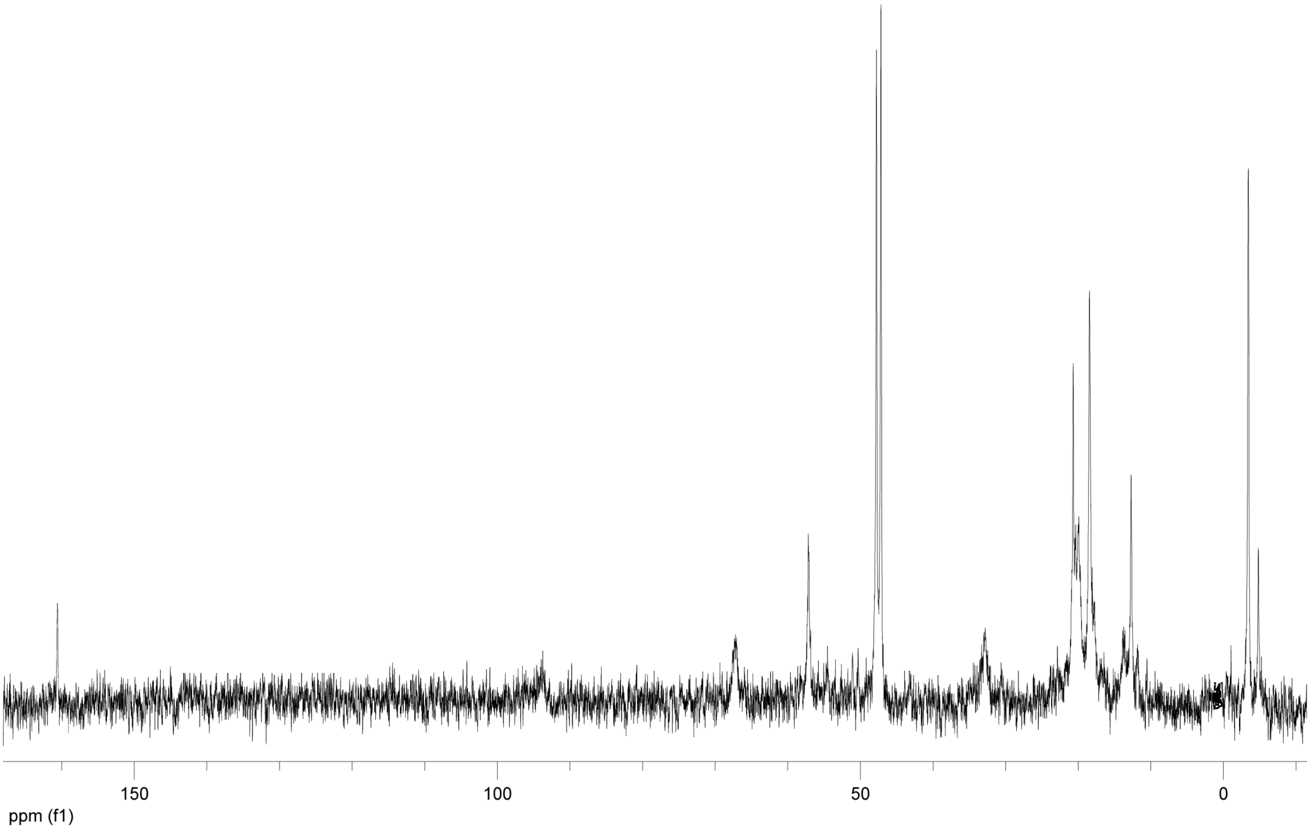

**Figure S25**. $^{13}$C NMR spectrum of $G_1O_3(C_2H_4SO_3Na)_{12}$ (**13**).

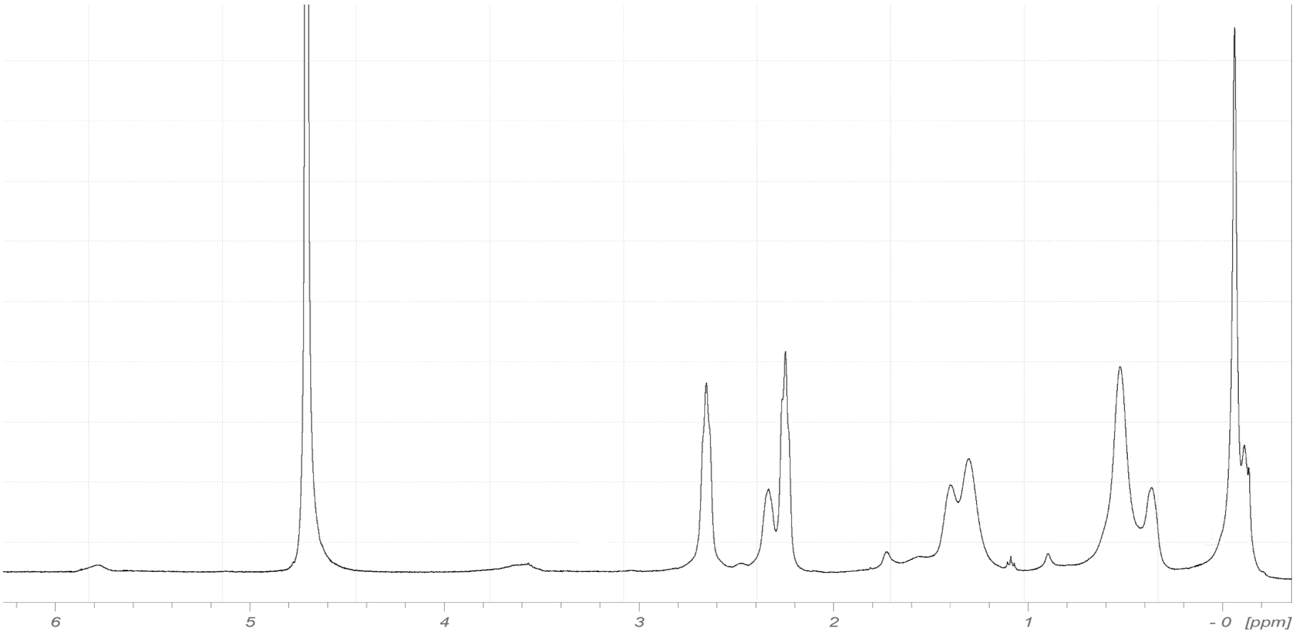

**Figure S26**. $^1$H NMR spectrum of $G_2O_3(C_2H_4CO_2Na)_{24}$ (**8**).

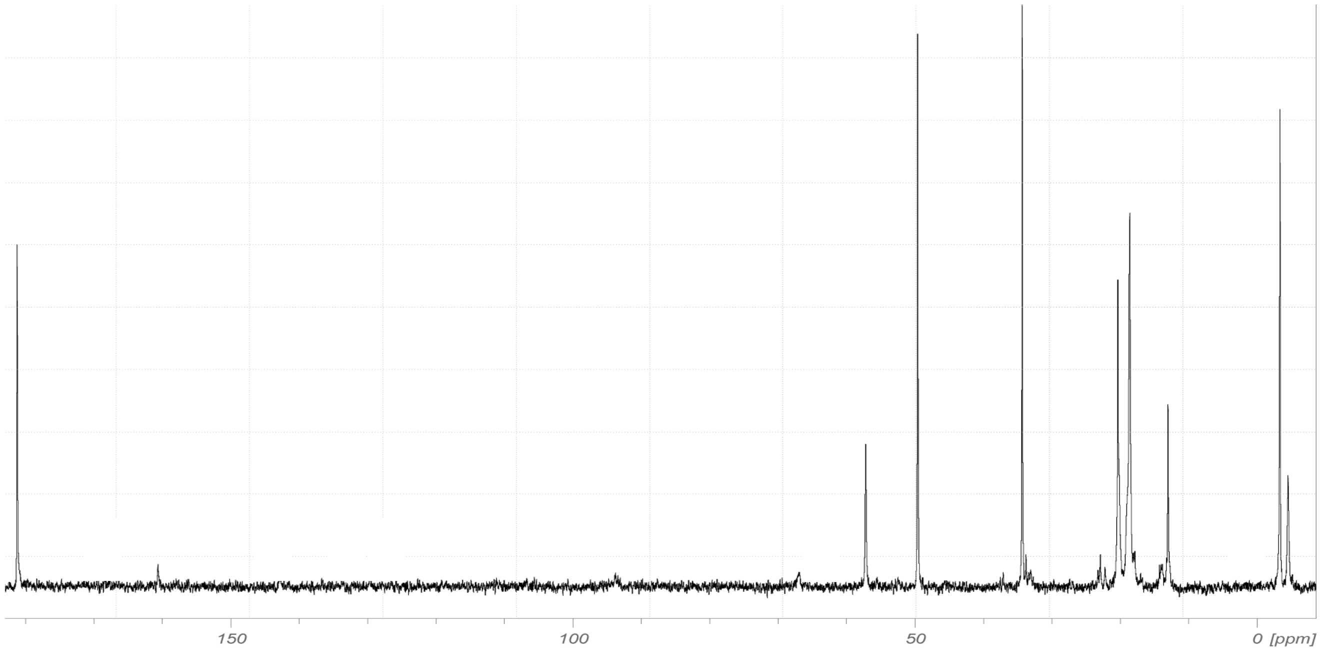

**Figure S27**. $^{13}$C NMR spectrum of $G_2O_3(C_2H_4CO_2Na)_{24}$ (**8**).

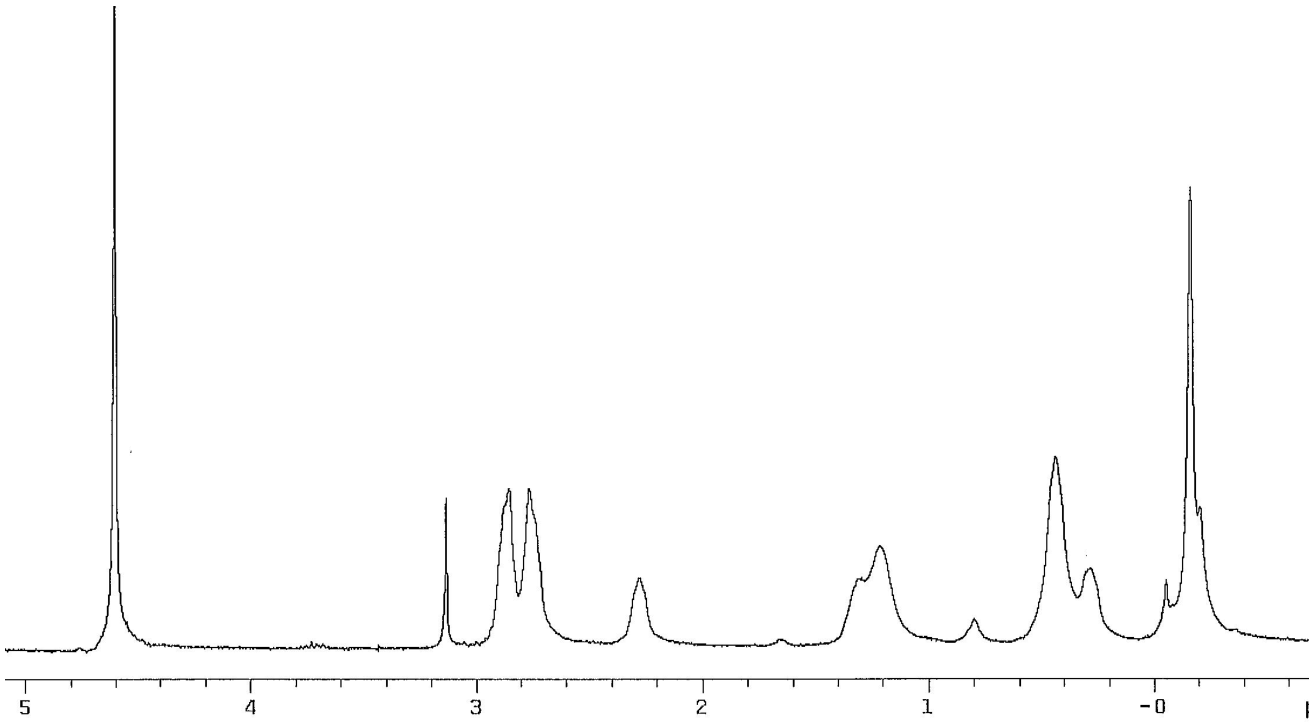

**Figure S28**. $^{1}$H NMR spectrum of $G_2Si(C_2H_4SO_3Na)_{16}$ (**17**).

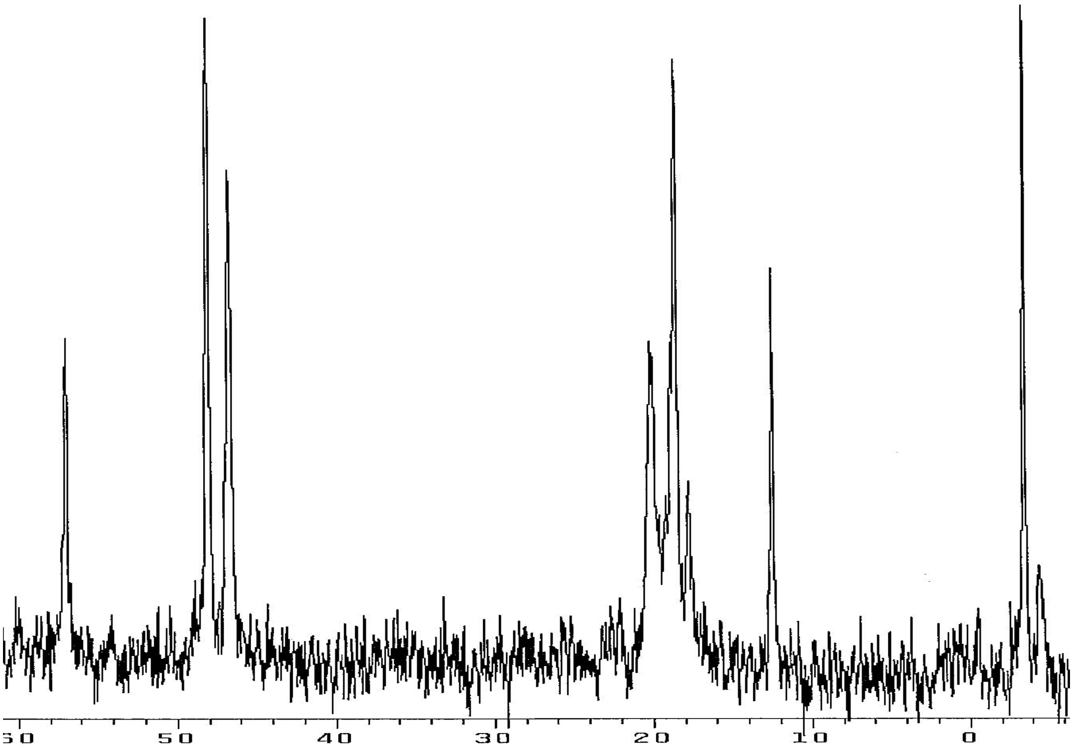

**Figure S29**. $^{13}$C NMR spectrum of $G_2Si(C_2H_4SO_3Na)_{16}$ (**17**).

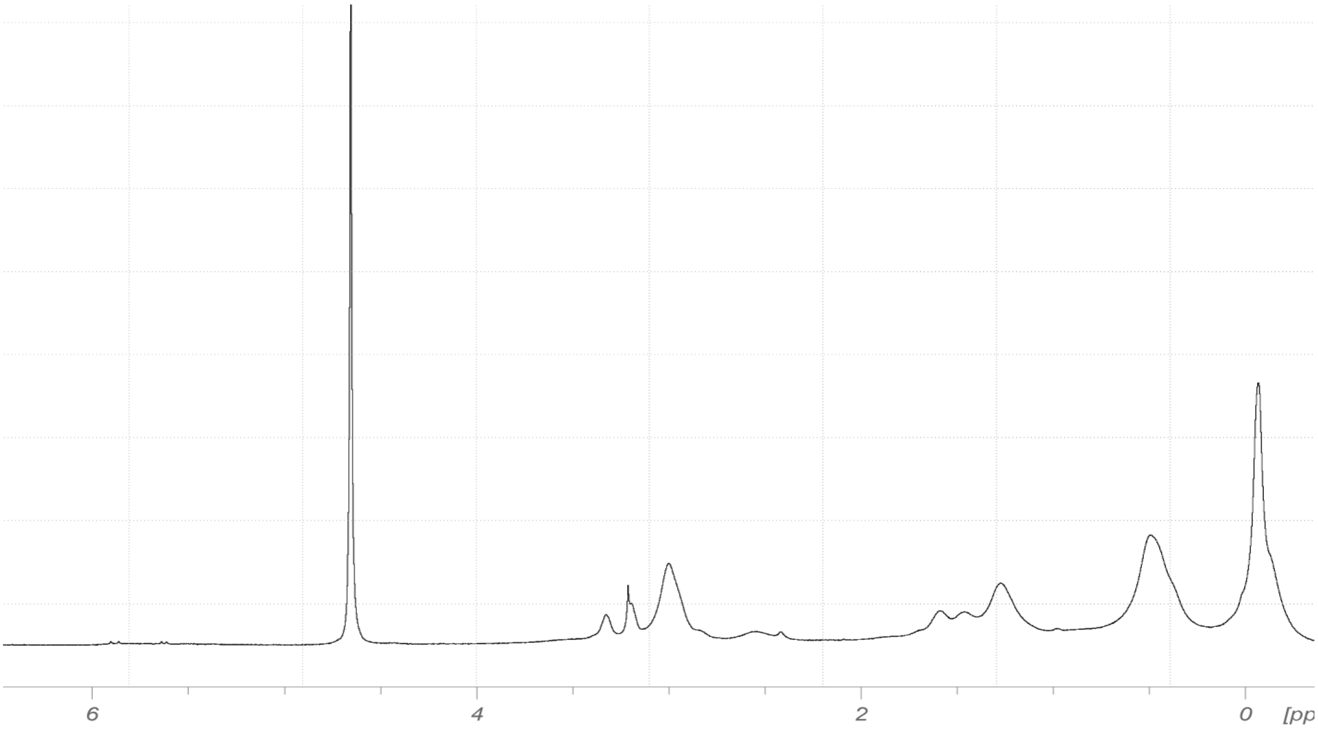

**Figure S30**. $^{1}$H NMR spectrum of $G_3O_3(C_2H_4SO_3Na)_{48}$ (**15**).

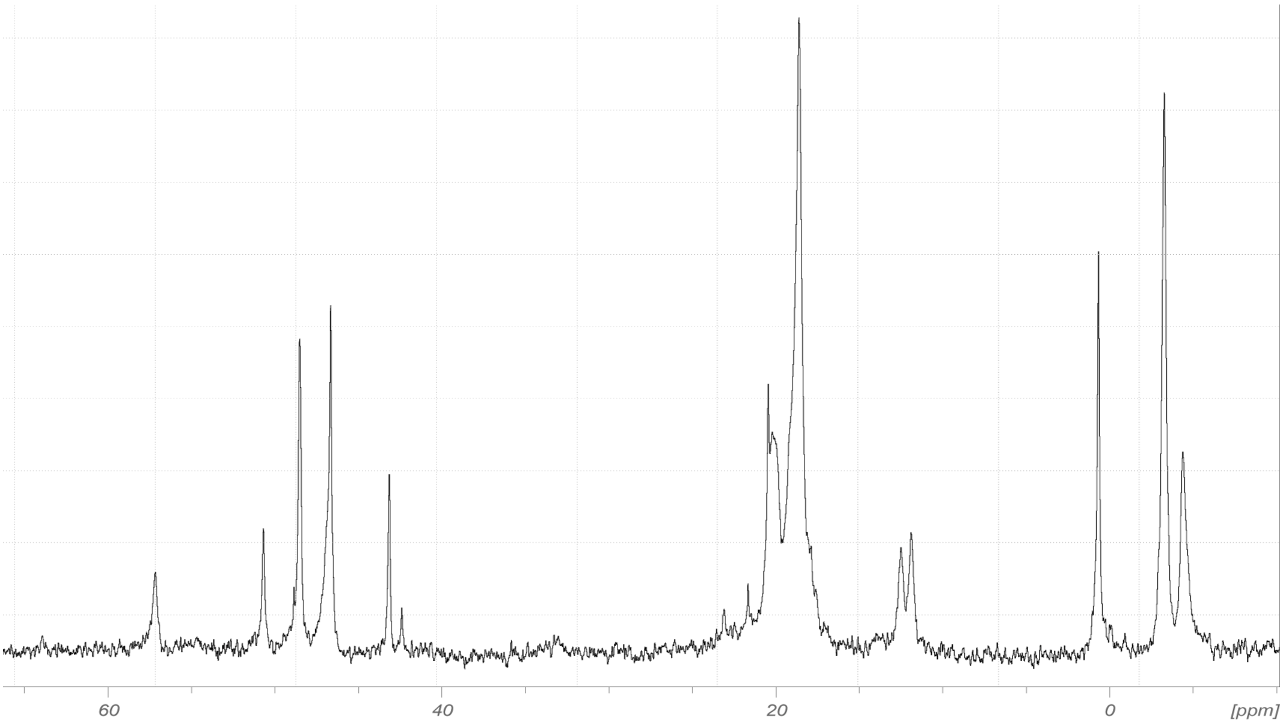

**Figure S31**. $^{13}$C NMR spectrum of $G_3O_3(C_2H_4SO_3Na)_{48}$ (**15**).

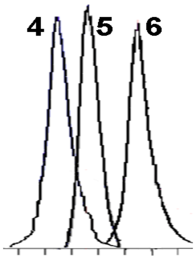

**Figure S32**. GPC of compounds **4-6**.

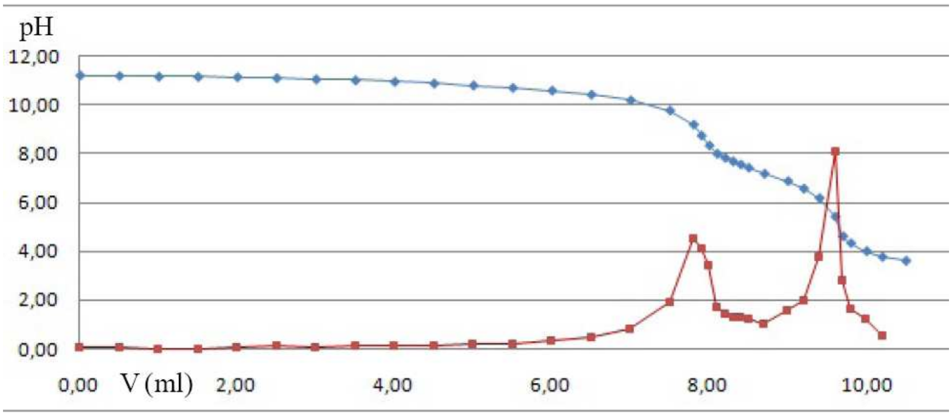

**Figure S33**. Titration curve (blue) and first derivative (red) of $G_0N(SO_3Na)_2$ (**D**).

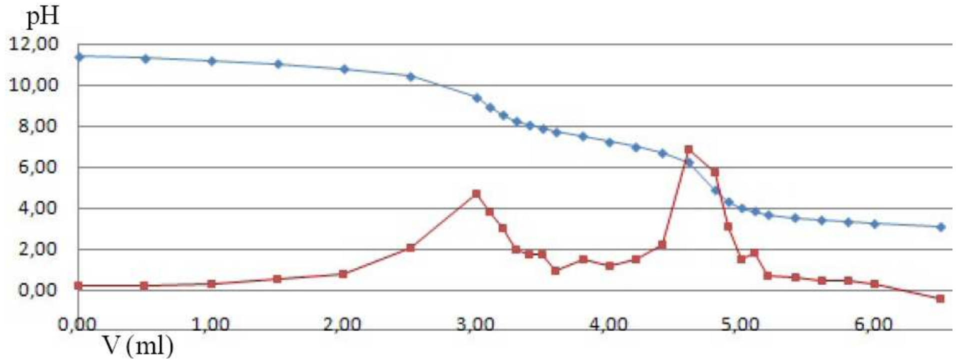

**Figure S34**. Titration curve (blue) and first derivative (red) of $G_0NH(SO_3Na)$ (**E**).

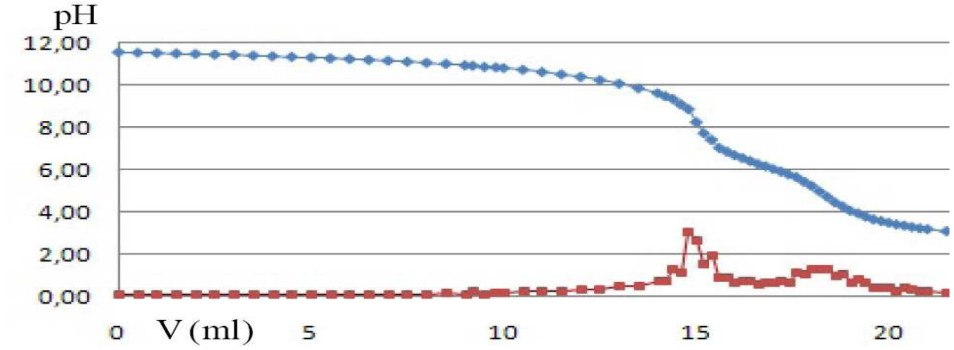

**Figure S35**. Titration curve (blue) and first derivative (red) of $G_2Si(CO_2Na)_{16}$ (**11**).

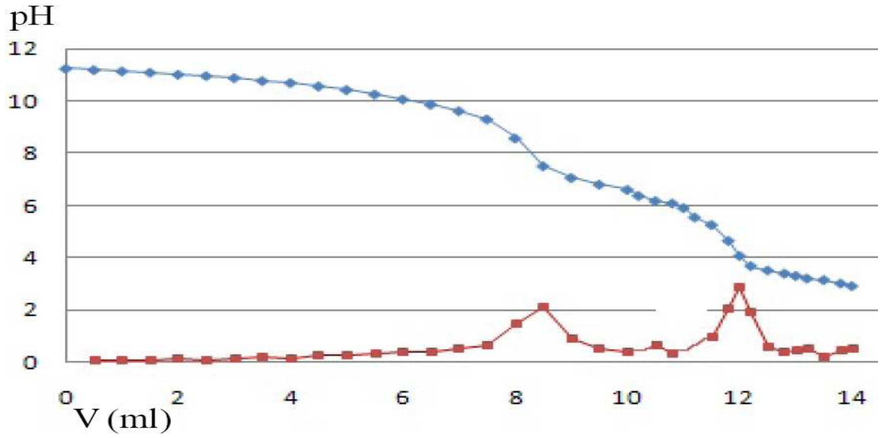

**Figure S36**. Titration curve (blue) and first derivative (red) of $G_2Si(SO_3Na)_{16}$ (**17**).